A Finite Element Method for Distortional Buckling Analysis of Thin-Walled Members

Sheng Jin

Xiao Jiana

Rui Chenga

Shidong Niea

Mingyue Chenga

Wei-Wen Yu International Specialty Conference on Cold-Formed Steel Structures
Baltimore, Maryland, U.S.A, November 9 & 10, 2016

A FINITE ELEMENT METHOD FOR DISTORTIONAL BUCKLING ANALYSIS OF THIN-WALLED MEMBERS

Sheng Jin[*,a,b], Xiao Jian[a], Rui Cheng[a,b], Shidong Nie[a,b], Mingyue Cheng[a]

(a. College of Civil Engineering, Chongqing University, Chongqing 400045, China; b. Key Laboratory of New Technology for Construction of Cities in Mountain Area (Chongqing University), Ministry of Education, Chongqing 400030, China)

Abstract

This paper presents a method for distortional buckling analysis of thin-walled members without assuming longitudinal shape of buckling modes. In this method, the pure distortional elastic buckling loads and deformation modes are achieved by performing a linear buckling analysis of a specially constrained finite element model of the thin-walled member in ANSYS. The constraints on each cross-section are applied independently and can be divided into two parts. The first part, by which distortional buckling can be distinguished from local buckling, depicts the transvers deformation of a cross-section, while the second part originated from longitudinal displacement patterns of distortional modes is used to distinguish this type of buckling from global buckling. Transverse membrane extensions are permitted in the proposed distortional buckling mode. A numerical example is given to demonstrate the method.

1. Introduction

Global or local buckled thin-walled members deform in flexural-torsional or local deformation modes respectively. These deformation modes are both familiar to us: flexural-torsional deformation is a mode where the member deforms without any distortion of the cross-section, while local deformation is characterized by the deformation of individual plate elements and no relative

[*]Corresponding author. Tel.: +86 13657688650; E-mail address: civiljs@cqu.edu.cn (Jin S).

translation of the fold-lines.

With the developments in cold-formed section technology, such as the reduction in thickness inspired by higher strength steels and the more complex sections with more folds and rolls in stiffeners, distortional buckling plays a more important role in failure of thin-walled members. This buckling mode takes place as a consequence of distortion of the cross-section. In cold-formed sections, it is characterized by relative translations of the fold-lines.

Distortional buckling mode used to be considered as coupled mode of global and local buckling modes, whereas its particularity is demonstrated by Generalized Beam Theory[14]: distortional deformation mode is proved to be orthogonal to flexural-torsional and local deformations. The typical mechanical properties of distortional deformation which are different from the other modes make distortional buckling individual.

The approach of modern design specifications to calculate the design stability capacity associated with distortional buckling, such as NAS 2007[1] and AS/NZS 2005[2], is to calculate the corresponding linear critical force first, then to consider the modification about post-buckling reserves, various kinds of imperfections and coupling with other buckling modes.

It is common to use GBT and FSM[6] to analyze linear distortional buckling of thin-walled members. The normal approach is to examine the minimum points of buckling curves, and the critical force of distortional buckling is determined by the minimum point at particular half-wave-length. However, that kind of point does not always exist[3], and even if it does exist, the buckling mode of that point contains not only distortional but also local/global deformation. Actually, the linear buckling totally in accordance with distortional deformation mode deduced by Generalized Beam Theory does not exist in common load conditions, and distortional deformation mode is usually coupled with global and especially local deformation modes.

Some researchers hold the point that the critical forces of pure deformation modes by artificial constraints in linear buckling analysis have more advantages to be used in stability capacity calculation.

2 Tools for research and developments into buckling phenomena

2.1 Generalized Beam Theory (GBT)

GBT[8][9][16][17][18] is important in pure distortional buckling mode research, for extracting distortional mode from deformations and providing with tools for analyzing mechanical properties of this kind of mode. Based on GBT, we can analyze linear buckling of any kind of deformation mode and proportions of pure modes in any deformation pattern.

2.2 Constrained Finite Strip Method (cFSM)

S. Ádány [3][4][10] introduced GBT's definitions of deformation modes into FSM and proposed cFSM. Constraints of pure modes and deformation modal decomposition of arbitrary buckling pattern are implemented. The ability to take into account transverse membrane extensions and shear deformations was developed, and corresponding deformation and buckling modes are proposed. A design approach has been proposed in which the elastic buckling results from pure mode cFSM are employed in the Direct Strength Method[14][19] for strength prediction

2.3 Finite Element Method (FEM)

FEM models have high adaptability of boundary conditions, and the stress-strain relation can be defined more precisely. Pure buckling mode analysis of thin-walled members cannot be performed by general-purpose FEM without definitions of pure deformation modes, therefore researchers have been studying in following fields.

S. Ádány et al. [11] translated the deformation mode defined in cFSM into FEM, then analyzed buckling modes calculated by FEM and figured out the percentage of participation of each mode (local, distortional, global, etc.). Thus modal identification and decomposition were achieved. They developed modal analyses with the benefit of FEM and discussed[12]: i)column with semi-rigid ends; ii) members with holes and irregular FEM mesh, iii) members undergoing thermal gradients; iv) nonlinear analysis.

Casafont M[5] derived the relation of fundamental modes, based on the deformation modes defined by GBT. In shell finite element analyses of thin-walled members, they draw the conclusion about linear buckling of pure deformation mode, where the deformation relation is defined by constraint equations.

Nedelcu M[13] presented a method based on GBT capable to identify the fundamental deformation modes of global, distortional or local nature, in general buckling modes provided by the shell finite element analyses of isotropic thin-walled members. By this method the participation of each fundamental buckling mode can be calculated.

2.4 The method proposed in this paper

All the buckling mode analysis methods listed above are based on results of GBT cross-section analysis, and longitudinal curve shapes of deformation modes have to be designated in most of them.

A new finite element procedure to carry out linear distortional buckling analysis of thin-walled members is developed in the next section. GBT cross-section analysis and longitudinal curve shapes of deformation modes are not required in this procedure, which is convenient for simplifying the process of linear buckling analysis.

3. Constraining a finite element mesh

3.1 Notation for the thin-walled members

A thin-walled open-section member is shown in Fig. 1: *u, v, w* are the displacements expressed in the local plate systems, the x–y–z coordinate systems; *U–V–W* and θ are the displacements corresponding to the global coordinate system, the X-Y-Z system.

As depicted in Fig. 1, the member consists of *n* thin rectangular plate walls, the width and thickness of plate $\boxed{r}$ among them are $b_{\boxed{r}}$ and $t_{\boxed{r}}$. Consequently, the mid-line of the cross-section comprises *n* segments, the intersection points and the end points of the segments are both designated as “main nodes” here. Of all the *m* main nodes, the two end points of the $\boxed{r}$-th segment are numbered *i* and *j*, for example.

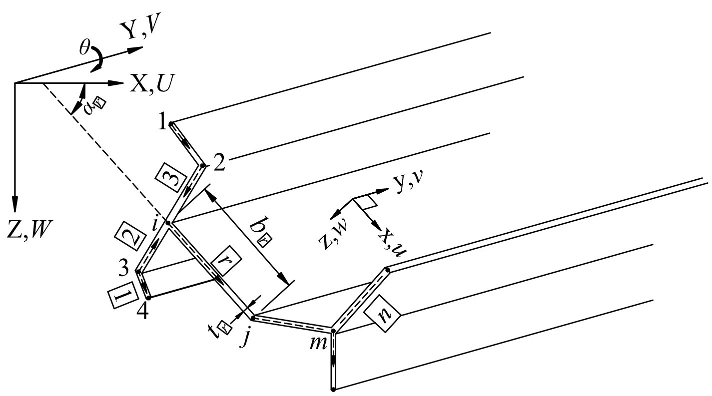

Fig. 1 A thin-walled open-profile member

3.2 Constraint equations to preclude torsional-flexural deformations

In GBT, the individual deformation modes are determined through a cross-section analysis process, involving mainly the constitution and solving of an eigenvalue problem containing two matrices. The purpose of this paper is to distinguish distortional mode from other deformation modes, instead of separating different distortional modes. As the result, the GBT cross-section analysis process is not required here. Nevertheless, the identification method of distortional buckling from global buckling, which is the orthogonality of longitudinal displacements, is adopted in this paper, with the assumption that longitudinal membrane displacements on a cross-section distribute lineally over the plate width and continuously at intersection points.

The orthogonality between distortional and torsional-flexural deformation is represented as:

$$\int_A V \cdot X_0 \mathrm{d}A = 0 \tag{1}$$

$$\int_A V \cdot Z_0 \mathrm{d}A = 0 \tag{2}$$

$$\int_A V \cdot \omega_0 \mathrm{d}A = 0 \tag{3}$$

where V is the longitudinal displacement of a point in distortional mode; X_0 and Z_0 are the coordinates of this point in the principal centroidal coordinate system; ω_0 is the principal sectorial coordinates of this point.

For the member in Fig. 1, Eq. (1), (2) and (3) can be written as follows:

$$\sum_{\boxed{r}} \left[\left(\frac{X_{0i}}{3} + \frac{X_{0j}}{6} \right) t_{\boxed{r}} b_{\boxed{r}} \cdot V_i + \left(\frac{X_{0i}}{6} + \frac{X_{0j}}{3} \right) t_{\boxed{r}} b_{\boxed{r}} \cdot V_j \right] = 0 \tag{4}$$

$$\sum_{\boxed{r}} \left[\left(\frac{Z_{0i}}{3} + \frac{Z_{0j}}{6} \right) t_{\boxed{r}} b_{\boxed{r}} \cdot V_i + \left(\frac{Z_{0i}}{6} + \frac{Z_{0j}}{3} \right) t_{\boxed{r}} b_{\boxed{r}} \cdot V_j \right] = 0 \tag{5}$$

$$\sum_{\boxed{r}} \left[\left(\frac{\omega_{0i}}{3} + \frac{\omega_{0j}}{6} \right) t_{\boxed{r}} b_{\boxed{r}} \cdot V_i + \left(\frac{\omega_{0i}}{6} + \frac{\omega_{0j}}{3} \right) t_{\boxed{r}} b_{\boxed{r}} \cdot V_j \right] = 0 \tag{6}$$

In each cross-section, Eq. (4), (5) and (6) compose an equation set about longitudinal displacements of main nodes:

$$\begin{pmatrix} C_{11} & C_{12} & C_{13} & C_{14} & \cdots & C_{1m} \\ C_{21} & C_{22} & C_{23} & C_{24} & \cdots & C_{2m} \\ C_{31} & C_{32} & C_{33} & C_{34} & \cdots & C_{3m} \end{pmatrix} \begin{pmatrix} V_1 \\ V_2 \\ V_3 \\ V_4 \\ \vdots \\ V_m \end{pmatrix} = \begin{pmatrix} 0 \\ 0 \\ 0 \end{pmatrix} \tag{7}$$

According to Eq. (15), we can arbitrarily select three non-collinear main nodes, Node 1, 2 and 3 for example in this cross-section, and regard their longitudinal displacements as dependency displacements determined by longitudinal displacements of other main nodes, which is:

$$\begin{pmatrix} V_1 \\ V_2 \\ V_3 \end{pmatrix} = -\begin{pmatrix} C_{11} & C_{12} & C_{13} \\ C_{21} & C_{22} & C_{23} \\ C_{31} & C_{32} & C_{33} \end{pmatrix}^{-1} \cdot \begin{pmatrix} C_{14} & \cdots & C_{1m} \\ C_{24} & \cdots & C_{2m} \\ C_{34} & \cdots & C_{3m} \end{pmatrix} \cdot \begin{pmatrix} V_4 \\ \vdots \\ V_m \end{pmatrix} \tag{8}$$

Constraint equations precluding global buckling can be defined according to Eq. (8). There are three equations for each cross-section.

3.3 Constraint equations to preclude local deformation

Although the plate walls bend in their out-of-plane direction in both local and distortional deformation modes, the two types of out-of-plane deformations are different and even orthogonal to each other. In order to shorten the calculation process correlate to such orthogonality, GBT and cFSM neglected the effects of longitudinal out-of-plane bending and its coupling with transverse bending, resulting in more simplified orthogonality of cross-sectional transverse deformation.

Cross-section of the thin-walled member is depicted in Fig. 2, which can also be looked on as an equivalent beam system: each beam's length and the depth of its cross-section are the width and thickness of corresponding plate, respectively, while their cross-section widths are the same, say, 1.

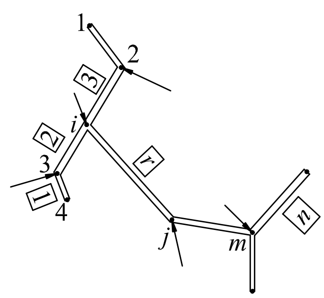

Fig. 2 Equivalent beam system

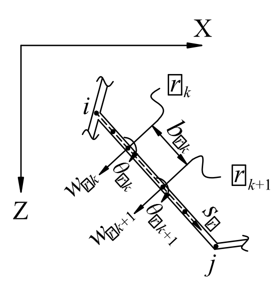

Fig. 3 Sub-divided beam r

The cross-sectional transverse deformations of the thin-walled member's local mode can be simulated by the beam system under arbitrary loads with all the intersection points pined. For the beam system, other deformation patterns orthogonal to that should be under concentrated forces applied arbitrarily on the intersection points. Consequently, the latter can be looked on as the cross-sectional transverse deformations in distortional mode of the thin-walled member.

In order to provide enough degree of freedom for the orthogonal analysis of the beam system's deformations, the beams is divided further with subordinate nodes. The sub-divided beam $\boxed{r}$ is depicted in Fig. 3, where the length of its segment k is $b_{\boxed{r}k}$ and the nodes at both ends are Node $\boxed{r}_k$ and Node $\boxed{r}_{k+1}$.

In GBT, the membrane transverse extensions of distortional mode are prescribed to be 0, but in shell elements, constraints on membrane transverse strains may result in undesired membrane longitudinal stresses. For that sake, a different way from cFSM is chosen in this paper, in which membrane transverse extensions are not constrained. In doing so, axial deformation functions of all elements are excluded in the analyses of the equivalent beam system.

Bending equations of segment k in beam $\boxed{r}$ are:

$$\begin{pmatrix} Q_{\boxed{r}k} \\ M_{\boxed{r}k} \\ Q_{\boxed{r}k+1} \\ M_{\boxed{r}k+1} \end{pmatrix} = \frac{t_{\boxed{r}}^3}{12\cdot(1-\nu^2)} \begin{pmatrix} 12/b_{\boxed{r}k}^3 & 6/b_{\boxed{r}k}^2 & -12/b_{\boxed{r}k}^3 & 6/b_{\boxed{r}k}^2 \\ 6/b_{\boxed{r}k}^2 & 4/b_{\boxed{r}k} & -6/b_{\boxed{r}k}^2 & 2/b_{\boxed{r}k} \\ -12/b_{\boxed{r}k}^3 & -6/b_{\boxed{r}k}^2 & 12/b_{\boxed{r}k}^3 & -6/b_{\boxed{r}k}^2 \\ 6/b_{\boxed{r}k}^2 & 2/b_{\boxed{r}k} & -6/b_{\boxed{r}k}^2 & 4/b_{\boxed{r}k} \end{pmatrix} \begin{pmatrix} w_{\boxed{r}k} \\ \theta_{\boxed{r}k} \\ w_{\boxed{r}k+1} \\ \theta_{\boxed{r}k+1} \end{pmatrix} \tag{9}$$

Synchronizing Eq. (9)s of all elements in the equivalent beam system, resulting in the global bending equations:

$$\begin{pmatrix} \boldsymbol{Q} \\ \boldsymbol{M} \end{pmatrix} = \boldsymbol{K} \begin{pmatrix} \boldsymbol{w} \\ \boldsymbol{\theta} \end{pmatrix} \tag{10}$$

where $\boldsymbol{w}$ and $\boldsymbol{\theta}$ are the deflections and rotation angles of all nodes; $\boldsymbol{Q}$ and $\boldsymbol{M}$ are the corresponding nodal forces.

Separate deflections on intersection nodes of beams, $\boldsymbol{w}_{\mathrm{IN}}$, from those of other nodes, $\boldsymbol{w}_{\mathrm{NN}}$, Eq. (10) can be rewritten as:

$$\begin{pmatrix} \boldsymbol{Q}_{\mathrm{IN}} \\ \hdashline \boldsymbol{Q}_{\mathrm{NN}} \\ \boldsymbol{M} \end{pmatrix} = \left(\begin{array}{c:c} \boldsymbol{K}_1 & \boldsymbol{K}_2 \\ \hdashline \boldsymbol{K}_3 & \boldsymbol{K}_4 \end{array}\right) \begin{pmatrix} \boldsymbol{w}_{\mathrm{IN}} \\ \hdashline \boldsymbol{w}_{\mathrm{NN}} \\ \boldsymbol{\theta} \end{pmatrix} \tag{11}$$

The $\boldsymbol{Q}_{\mathrm{NN}}$ and $\boldsymbol{M}$ are zeroes in distortional deformation mode, which lead to:

$$\begin{pmatrix} \boldsymbol{w}_{\mathrm{NN}} \\ \boldsymbol{\theta} \end{pmatrix} = -\boldsymbol{K}_4^{-1}\boldsymbol{K}_3\boldsymbol{w}_{\mathrm{IN}} \tag{12}$$

For any node, the deflection, w, can be determined by that node's translation in X-axis and Z-axis, U and W. For example:

$$w_{\boxed{r}k} = -\cos\alpha_{\boxed{r}} U_{\boxed{r}k} + \sin\alpha_{\boxed{r}} W_{\boxed{r}k} \tag{13}$$

where $\alpha_{\boxed{r}}$ is the angle between x-axis of Plate $\boxed{r}$ and X-axis of the global coordinate system, as depicted in Fig. 1. By substituting Eq. (13) into Eq. (12), the constraint equations precluding local deformation mode from distortional mode can be expressed as Eq. (14) and (15):

$$-\cos\boldsymbol{\alpha}_{\mathrm{NN}}\boldsymbol{U}_{\mathrm{NN}} + \sin\boldsymbol{\alpha}_{\mathrm{NN}}\boldsymbol{W}_{\mathrm{NN}} = \boldsymbol{D}_1\begin{pmatrix}\boldsymbol{U}_{\mathrm{IN}}\\ \boldsymbol{W}_{\mathrm{IN}}\end{pmatrix} \tag{14}$$

$$\boldsymbol{\theta} = \boldsymbol{D}_2\begin{pmatrix}\boldsymbol{U}_{\mathrm{IN}}\\ \boldsymbol{W}_{\mathrm{IN}}\end{pmatrix} \tag{15}$$

Eq. (14) is transplacement constraints of all non-intersection nodes in normal direction of plane, and Eq. (15) is the constraints of all nodes' rotation angle about Y-axis. They are determined by transverse displacements of intersection nodes in their same cross-section.

Note that shell element in FE analysis may use the method of incompatible modes to enhance the accuracy in bending-dominated problems. In the cases where the mesh is coarse, incompatible modes may perform incorrectly with the constraint equations of rotation angles, which leads to an inaccurate result. Therefore the Eq. (14) is applied as constraint equations of distortional mode to preclude local mode without Eq. (15).

4. Numerical example

A uniformly compressed channel member with the section depicted in Fig. 4 is considered. The thickness of plates is 2mm, the Young's modulus is 206kN/mm^2, and the Poisson's ratio is 0.3.

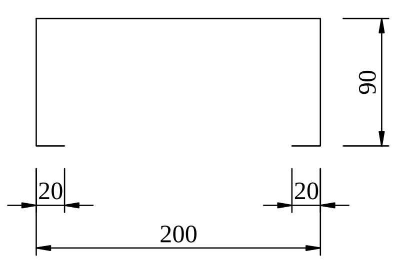

Fig. 4 Geometry of the cross-section (dimensions in mm)

A shell FE buckling analysis of the thin-walled member was performed in ANSYS, using SHELL181 element in a rectangular mesh. The full integration option of SHELL181 element is applied, for increasing the accuracy of the computation of in-plane bending. The cross-section discretization is made with 1, 3 and 0 intermediate nodes between the corners in the flanges, web and flange lips respectively.

During the process of linear buckling analysis in ANSYS, constraint equations (8) and (14) are applied to the model to force the mesh to buckle in distortional deformation mode.

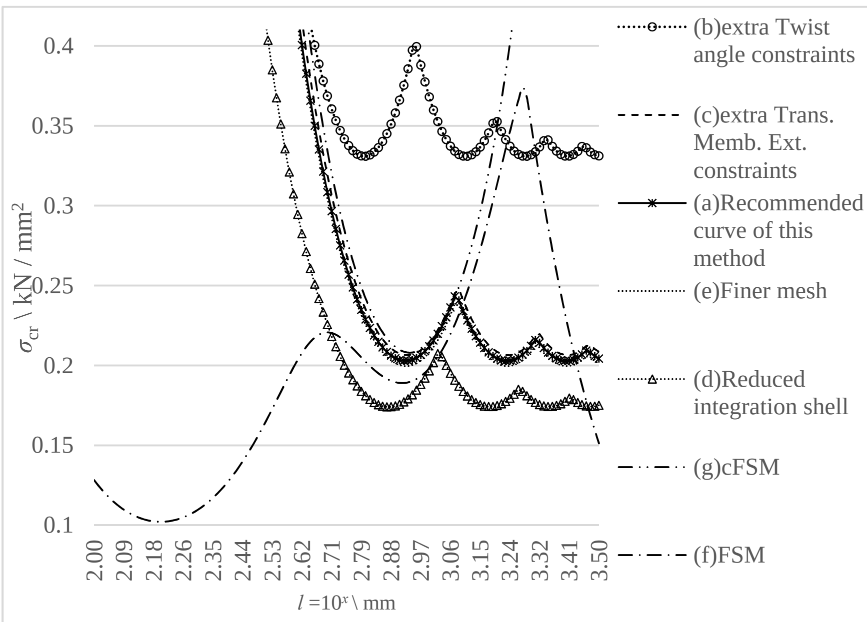

Fig. 5 Curves of critical stress

The resulting critical stress curve (a) is depicted in Fig. 5 with results of all deformation modes (f) and distortional modes (g) calculated by CUFSM[7], both in one-half sine wave.

Several other results are also plotted as curve (b)-(e), using the same method and mesh of modal as curve (a) with the differences that: extra axial twist constrain equations according to Eq. (15) are included in (b); extra constraints of transverse membrane extensions are considered in (c); uniform reduced but not the full integration mode option of shell SHELL181 element is applied in (d); relatively well-refine discretization is made in (e), with 3, 9 and 3 intermediate nodes between the corners in the flanges, web and flange lips, respectively.

Fig. 6 demonstrates that i) result of (b) is much higher than the others, as mentioned in last section, and ii) result of (d) is much lower in magnitude than the others, due to the errors of SHELL181 element's reduced integration option in coarse mesh.

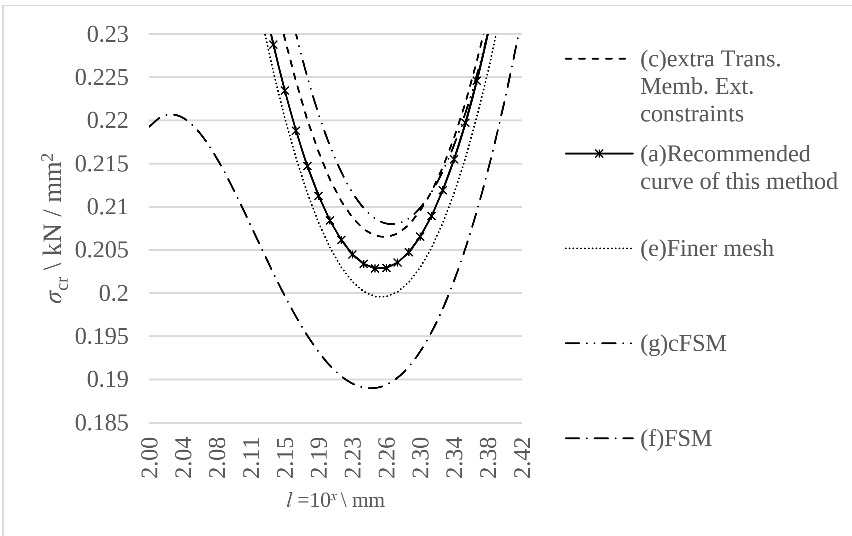

Fig. 6 Curves of critical stress near the minimum points

Curve (a), (c) and (e) are nearly the same with distortional mode of cFSM. These curves near their minimum points are plotted in a larger scale in Fig. 6. It shows that the method in this paper can reach sufficiently accurate results even with the FE meshed coarsely. In addition, the effects of transverse membrane extension constraints on critical loads of distortional mode should not be neglected.

5. Conclusion

A new method forcing the shell finite element models to deform in distortional mode with constraint equations is provided here. The constraints on each cross-section are applied independently. They can even be separated into two parts, and the constraints of transverse displacements are not coupled with those of longitudinal displacements. This method is not on the basis of GBT cross-section analysis procedure, therefore the implement of it is relatively convenient.

The use of shell elements for modeling thin-walled members in FEM is common. While the mesh is coarse, options of shell elements should be carefully chosen and examined for a more accurate result.

In order to take into account the impacts of some strains used to be neglected, such as transverse membrane extension and shear strain, usual solution is to define new deformation modes according to those strains, then to consider the coupling of new modes with original modes in buckling analysis. Another solution is discussed in this paper: adding those strain into original modes such as distortional mode, which is convenient for simplifying the process of linear buckling analysis.

Acknowledgments

The support of this work by the Fundamental Research Funds for the Central Universities (Nos. 106112015CDJXY200001, CDJRC11200002) and Natural Science Foundation Project of CQ CSTC (No. cstc2012jjA30004) is gratefully acknowledged.

References

[1] AISI. North American Specification for the Design of Cold-Formed Steel Structural Members (2007 Edition). Washington(DC, USA); 2007.

[2] Australian/New Zealand Standard, AS/NZS 4600, Cold-Formed Steel Structures, 2005.

[3] Ádány S. Buckling mode classification of members with open thin-walled cross-sections by using the Finite Strip Method. Research Report, Johns Hopkins University; 2004.

[4] Ádány S, Schafer BW. A full modal decomposition of thin-walled, single-branched open cross-section members via the constrained finite strip method. Journal of Constructional Steel Research, 2008, 64(1):12-29.

[5] Casafont M, Marimon F, Pastor M, Ferrer M. Linear buckling analysis of thin-walled members combining the Generalized Beam Theory and the Finite Element Method. Computers & Structures. 2011;89(21–22):1982-2000.

[6] Cheung YK, Tham LG. The finite strip method. CRC Press; 1998.

[7] CUFSM. Elastic Buckling Analysis of Thin-walled Members with general end boundary conditions. CUFSM 2012; v4.05. http://www.ce.jhu.edu/bschafer/cufsm.

[8] Davies JM, Leach P. First-order generalized beam theory. Construct. Steel Res. 1994,31(2–3):187–220.

[9] Davies JM, Leach P, Heinz D. Second-order generalized beam theory. Construct. Steel Res. 1994,31(2–3):221–41.

[10] Li Z, Hanna MT, Ádány S, Schafer BW. Impact of basis, orthogonalization, and normalization on the constrained Finite Strip Method for stability solutions of open thin-walled members. Thin-Walled Structures. 2011, 49(9): 1108-22.

[11] Li Z, Ádány S, Schafer BW. Modal identification for shell finite element models of thin-walled members in nonlinear collapse analysis. Thin-Walled Structures. 2013, 67: 15-24.

[12] Li ZJ, Abreu JCB, Leng JZ, Adany S, Schafer BW. Review: Constrained finite strip method developments and applications in cold-formed steel design. Thin-Walled Structures. 2014, 81:2-18.

[13] Nedelcu M, Cucu HL. Buckling modes identification from FEA of thin-walled members using only GBT cross-sectional deformation modes. Thin-Walled Structures. 2014, 81:150-8.

[14] Schafer BW. Review: The Direct Strength Method of cold-formed steel member design. Journal of Constructional Steel Research. 2008;64(7–8):766-78.

[15] Schardt R. Generalized beam theory - an adequate method for coupled stability problems. Thin-Walled structures 1994, 19(2-4); 161-180.

[16] Silvestre N, Camotim D. First-order generalized beam theory for arbitrary orthotropic materials.[J]Thin-Walled Struct 2002, 6:749–83.

[17] Silvestre N, Camotim D. Second-order generalized beam theory for arbitrary orthotropic materials.[J]Thin-Walled Struct 2002, 40:785–814.

[18] Silvestre N, Camotim D. Distortional buckling formulae for cold-formed steel C and Z-section members: partI—derivation. Thin Wall Struct, 2004,42(11):1567–97.

[19] Yu WW. Cold-formed steel design. John Wiley & Sons, Inc.; 2000.